ICWE14 June 21-26, 2015 | Porto Alegre - Brazil 14th INTERNATIONAL CONFERENCE ON WIND ENGINEERING

Wind tunnel study of wind loads on a tennis stadium open roof

Marañón Di Leo, J.[1,2], Delnero, J.S.[1,2], Scarabino, A[3], Garcia Saínz, M.O.[1,2]

[1]UIDET Capa Límite y Fluidodinámica Ambiental (UIDET LaCLyFA), Universidad Nacional de La Plata, La Plata, Argentina
[2]Consejo Nacional de Investigaciones Científicas y Técnicas, Cdad. de Buenos Aires, Argentina.
[3]UIDET Grupo de Fluidodinámica Computacional (UIDET GFC), Universidad Nacional de La Plata, La Plata, Argentina
email: jmaranon@ing.unlp.edu.ar, delnero@ing.unlp.edu.ar, scarabino@ing.unlp.edu.ar, mariano.garciasainz@ing.unlp.edu.ar

ABSTRACT: This paper aims to show the wind tunnel study of a roof for a tennis stadium, composed of a fixed and a sliding part. The need for this study is originated in the absence of information in the Argentinian codes for this type of roofs and the importance of a concrete knowledge of the wind effects on it for the determination of design loads on the involved structures. The results show a significant variability of loads, as expected, at different opening conditions of the sliding roof.

KEY WORDS: Open roof, wind loads, wind tunnel

1 INTRODUCTION

The Argentine code CIRSOC 102 [1] specifies some design loads for closed and permeable roofs, but it also recommends wind tunnel tests for non-standard structures. Wind loads on large roofs, as in sport stadiums, are a critical structural design factor. As Biagini et al point out, “every single structure is often a new ´study case´, so that a careful and thorough analysis of the design loads requires wind tunnel tests” [2].

A curved roof with a central sliding top, that can be either open or closed, is to be built above an existing tennis stadium. A gap between the roof and the stadium envelope allows some air to flow under the roof. The flow configuration and pressure distribution depend strongly on the roof opening. The objective of this work is to study through wind tunnel tests the flow configurations and, at this stage, the steady mean wind loads on this roof for different opening conditions.

2 METHODOLOGY

2.1. Stadium roof model

A 1:150 model of the stadium and its roof were built separately, in plywood and high impact polystyrene (Figure 1). Ninety-six pressure taps were distributed on both sides of eight roof panels, covering half of the model roof (Figure 2). Due to symmetry, these were enough to obtain the whole roof pressure distribution and resultant forces, by rotating the model 180 degrees and taking two sets of measurements for each wind direction and roof opening condition.

Experiments were carried out for three roof configurations: closed, open and semi-open, as shown in Figure 2, for the prevailing wind directions North, North-East and East. Another parameter to consider was the possibility of suppressing two glass panels that close the vertical gap between the supporting arc (shown in Figure 1) and the rest of the roof. Therefore a second set of experiments was carried out without these panels.

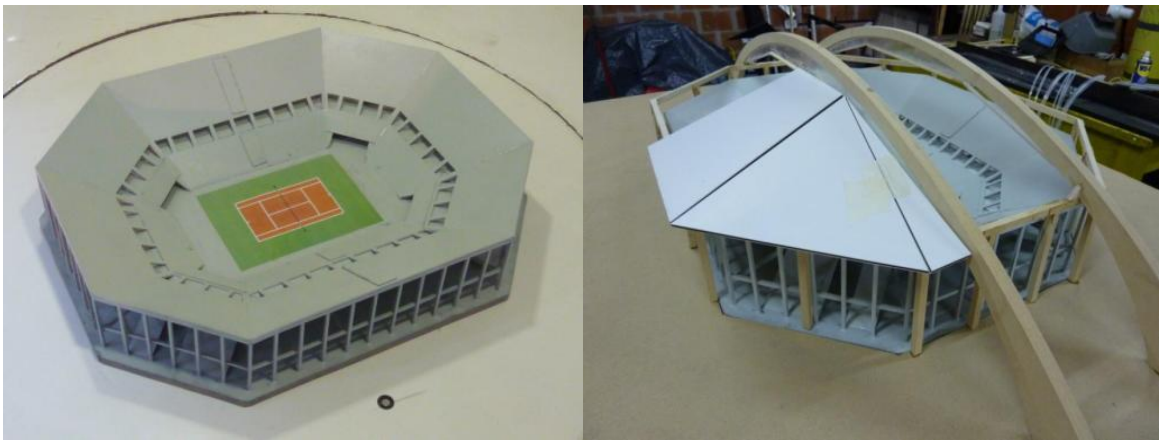

Figure 1. Stadium and roof models

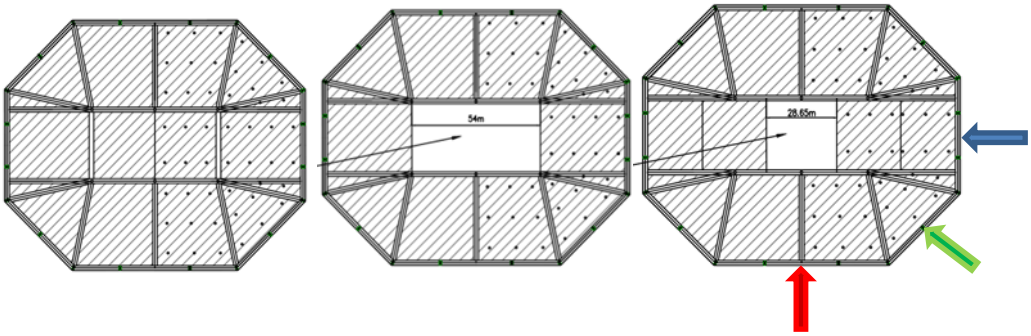

Figure 2. Tested roof configurations: closed, open and semi-open. (Wind direction [V_0]: Red arrow – East, Green arrow – North East, Blue arrow – North)

The experiments were carried out at the Boundary Layer and Environmental Fluid Dynamics Laboratory (LaCLyFA) at the Faculty of Engineering at the Universidad Nacional de La Plata, Argentina. The low atmospheric boundary layer was simulated by means of roughness elements on the tunnel floor, as shown in Figure 3. The boundary layer test section is 2.63 m wide, 1.83 m high and 12 m long. The velocity distribution was fitted with a power-law of exponent 0.12 (Figure 4).

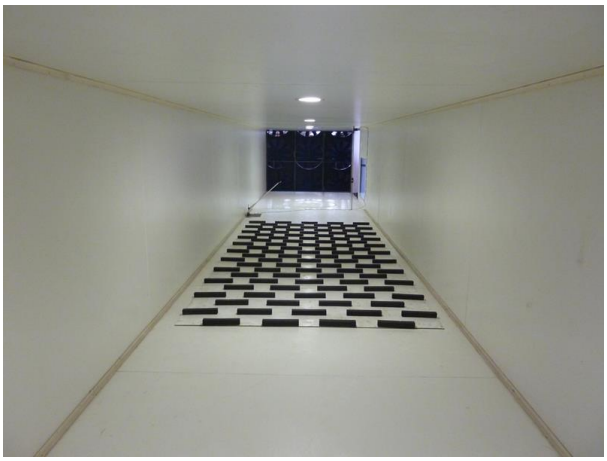

Figure 3. Roughness elements in the wind tunnel.

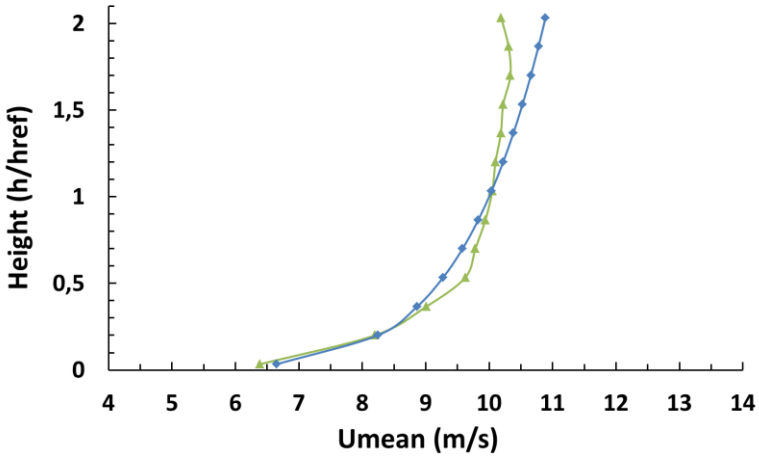

Figure 4. Umean velocity distribution (href = 30 cm.).

2.2 Pressure measurements and flow visualization

A "Testo 512" anemometer was used for checking the reference velocity. The pressure at the 96 roof taps was measured by a multimanometer "Net Scanner System". The test model was mounted on a turntable, allowing any wind direction to be simulated by rotating the model to the appropriate angle in the wind tunnel.

The measurements were taken for three prevailing wind directions: N, NE and E. The measured data were then converted into the form of pressure coefficients based on the measured mean dynamic pressure at the reference height. For each tap 500 samples at 3 Hz were taken and averaged to obtain the local mean pressure. This procedure was carried out for the roof open, semi-open and closed. Pressures for each tap were made non-dimensional as

$$C_{p_i} = \frac{P_i - P_{ref}}{q_i} \tag{1}$$

$$q_i = \frac{1}{2}\rho_i V_o^2 \tag{2}$$

Here ρ_i is the air density corrected by temperature in the wind tunnel, P_{ref} the atmospheric pressure and V_o the reference velocity of 15 m/s. The non-dimensional pressure difference between the outer and the inner side of the roof was computed for each tap pair as the difference: ΔC_p = *inner* C_p – *outer* C_p. Therefore, positive values of ΔC_p imply upward lift forces, and the opposite for negative ΔC_p. For computation of design loads, these nondimensional coefficients were then multiplied by the dynamic pressure corresponding to Buenos Aires reference wind design velocity of 45 m/s [1]. A second configuration was also tested, without the glass vertical panels.

For flow visualization, smoke was injected in the flow upstream of the model. For better visualization the reference velocity was reduced to 2 m/s. These tests were performed only for the model without glass panels.

In Figure 5 we show the lay out of the pressure tap distribution and the panel number identification. Because of the geometric symmetry of the roof model, only one half was instrumented. In order to get the complete pressure distribution, the model was rotated 180º and two data sets were acquired and processed for each wind direction.

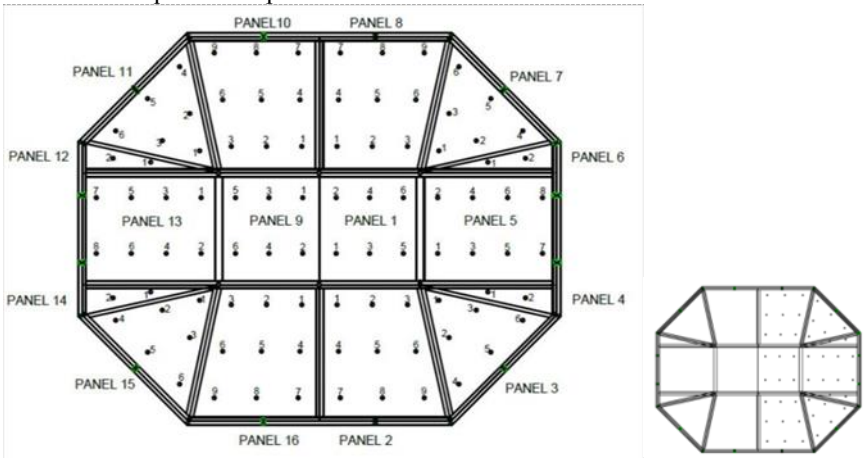

Figure 5: Panels identification and pressure tap distribution.

Figure 6 shows the vertical glass panels, which close the gap between the supporting arc of the sliding roof and the main roof.

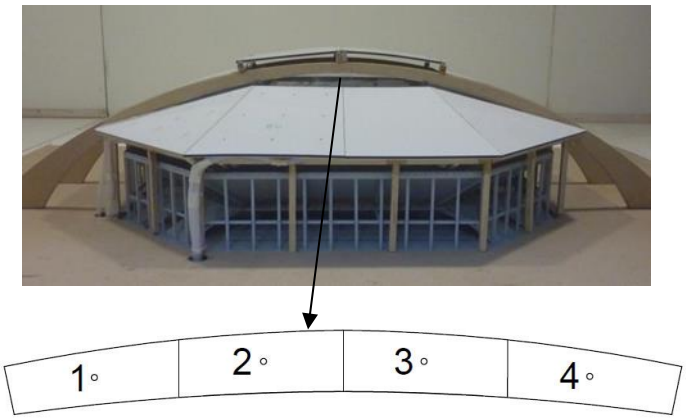

Figure 6. Glass panels identification and pressure tap distribution.

3 RESULTS

3.1. Flow visualization (no glass panels)

Figure 7 and Figure 8 show the flow configuration for different wind directions and roof opening conditions, without glass panels. A remarkable difference produced by opening the roof is the strong flow detachment at the top, caused apparently by the flow that enters under the roof on the windward side and exits through the roof opening.

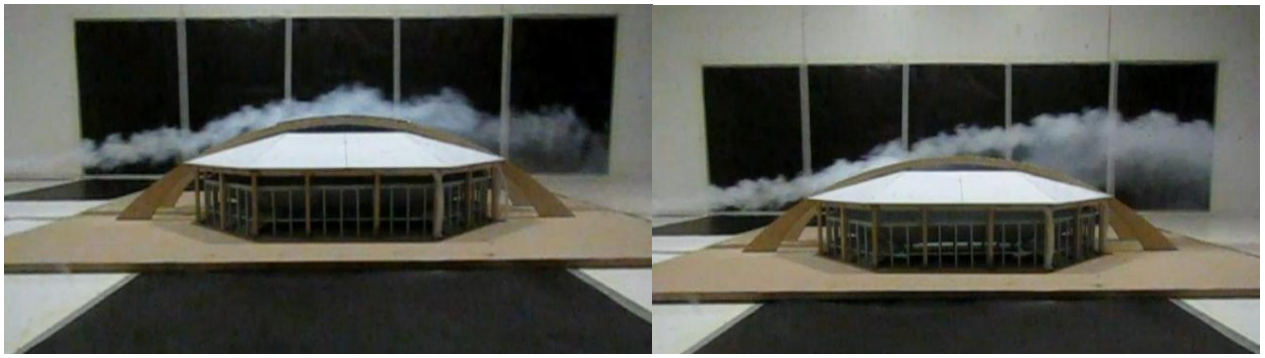

Figure 7. North Wind - Roof closed (left) and open (right)

Figure 8. East Wind – Roof closed (left) and open (right)

3.2 Distribution of ΔC_p – with glass panels

The worst condition for these panels, which determines the design loads, was found to be under Eastern winds. Nondimensional pressure differences acting on the points shown in Figure 6 are presented in Table 1.

Table 1. ΔC_p values on the glass panels for East wind.

Tap position	$\boldsymbol{\Delta C_p}$
1	-0.96
2	-1.02
3	-0.99
4	-0.80
Mean value	**-0.94**

Figure 9, Figure 10 and Figure 11 show the distribution of non-dimensional pressure differences for different wind directions and roof openings, for the configuration with lateral glass panels. It can be seen that for all wind directions the open roof reduces the maximum local loads.

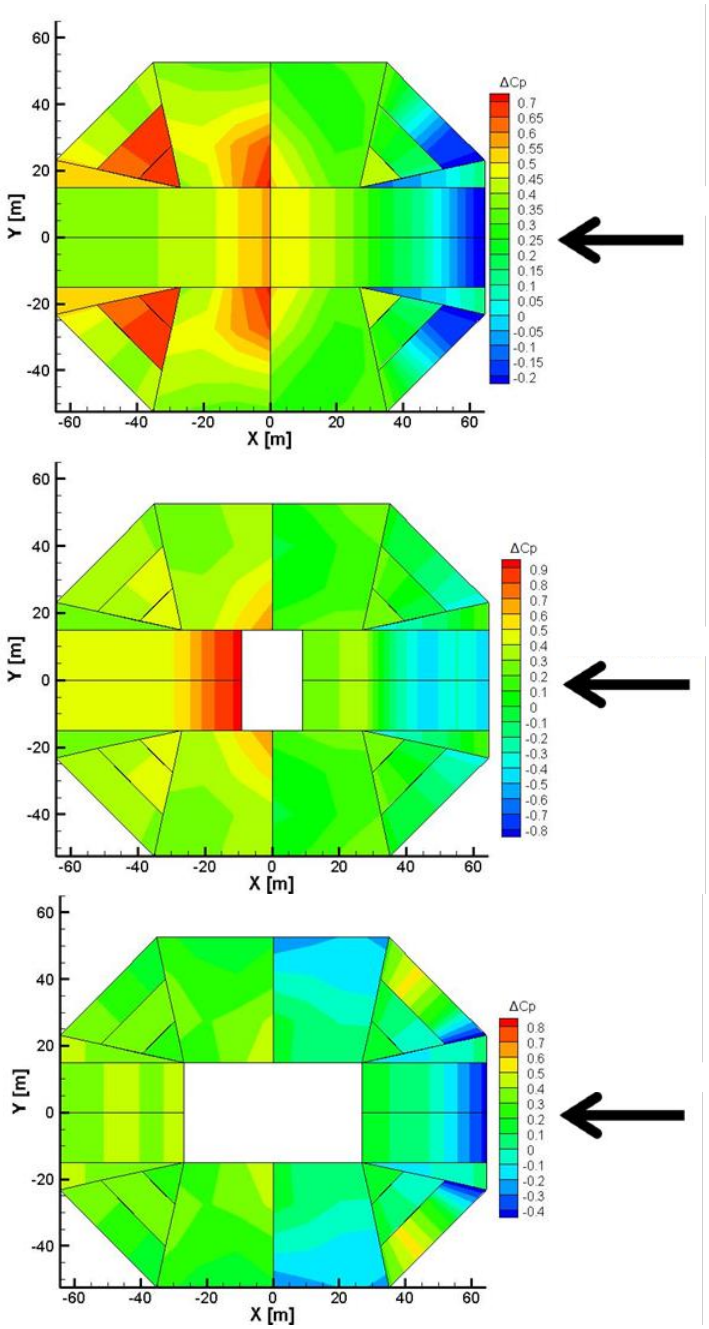

Figure 9. ΔC_p distribution – North Wind.

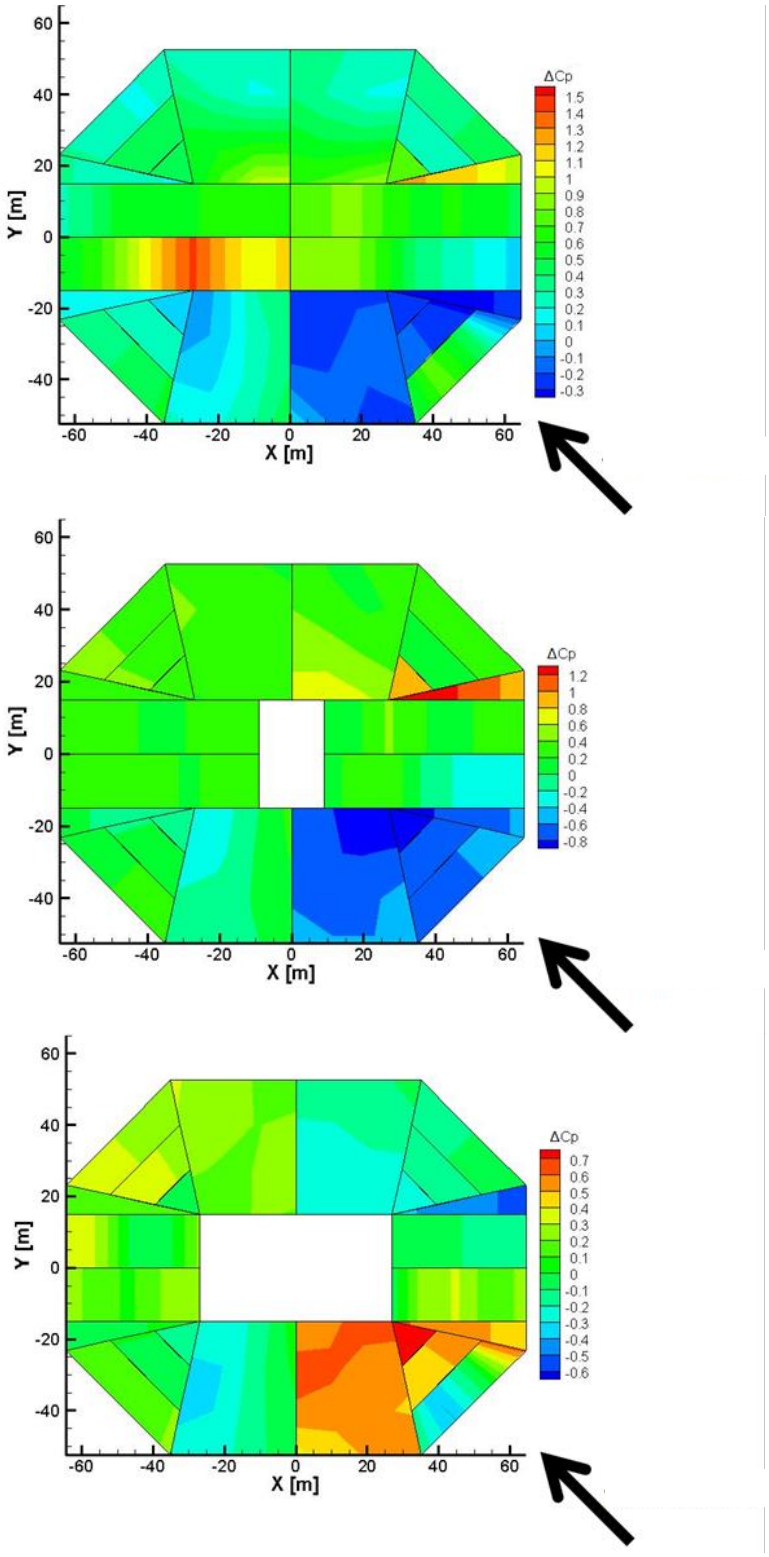

Figure 10. ΔC_p distribution – North-East Wind.

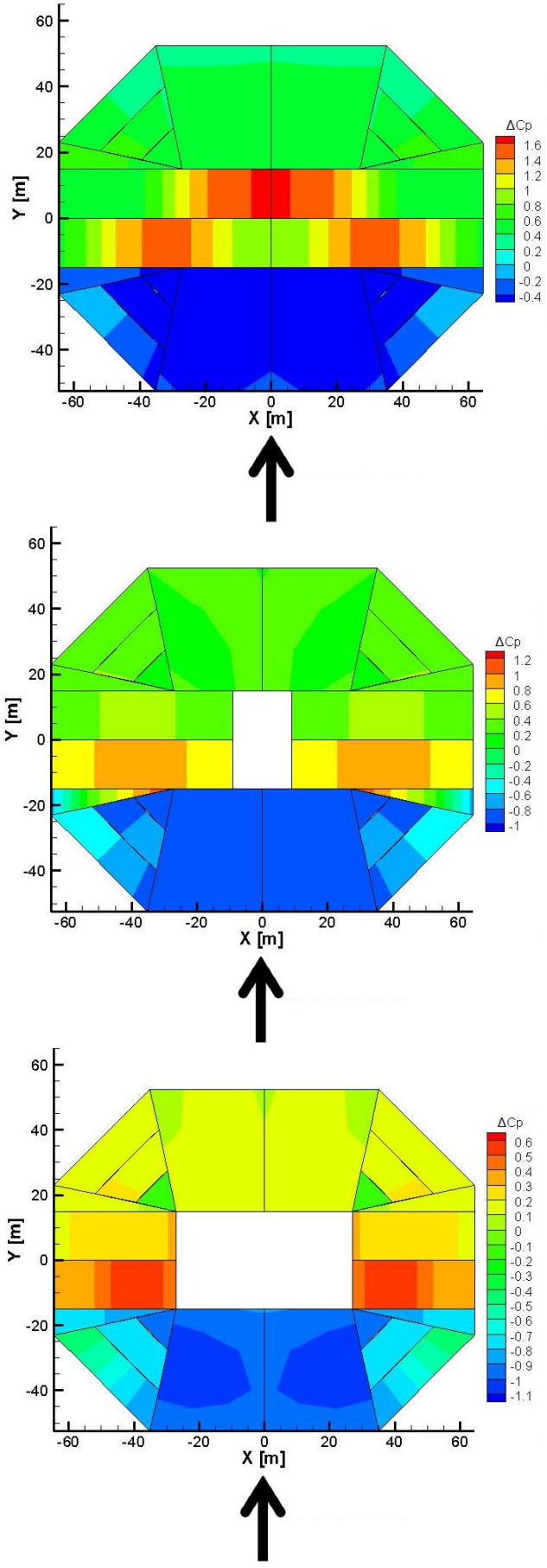

Figure 11. ΔC_p distribution – East Wind.

Nevertheless, the effect on each roof panel local loads varies. In Table 2, Table 3 and Table 4 maximum pressure loads were derived from the measured nondimensional coefficients, for the reference design velocity of Buenos Aires City, 45 m/s after [1]. For example, in Table 1 whereas the maximum pressure difference is reduced for the open roof, negative pressure differences on panels 2, 3 and 4 and their symmetrical ones reach higher values than for the case of the closed roof.

In all cases, it can be seen that the effect of opening the roof is different for each roof panel, increasing the loads in some of them when compared with the closed roof, and reducing the loads for others, thus reinforcing the importance of this experimental study.

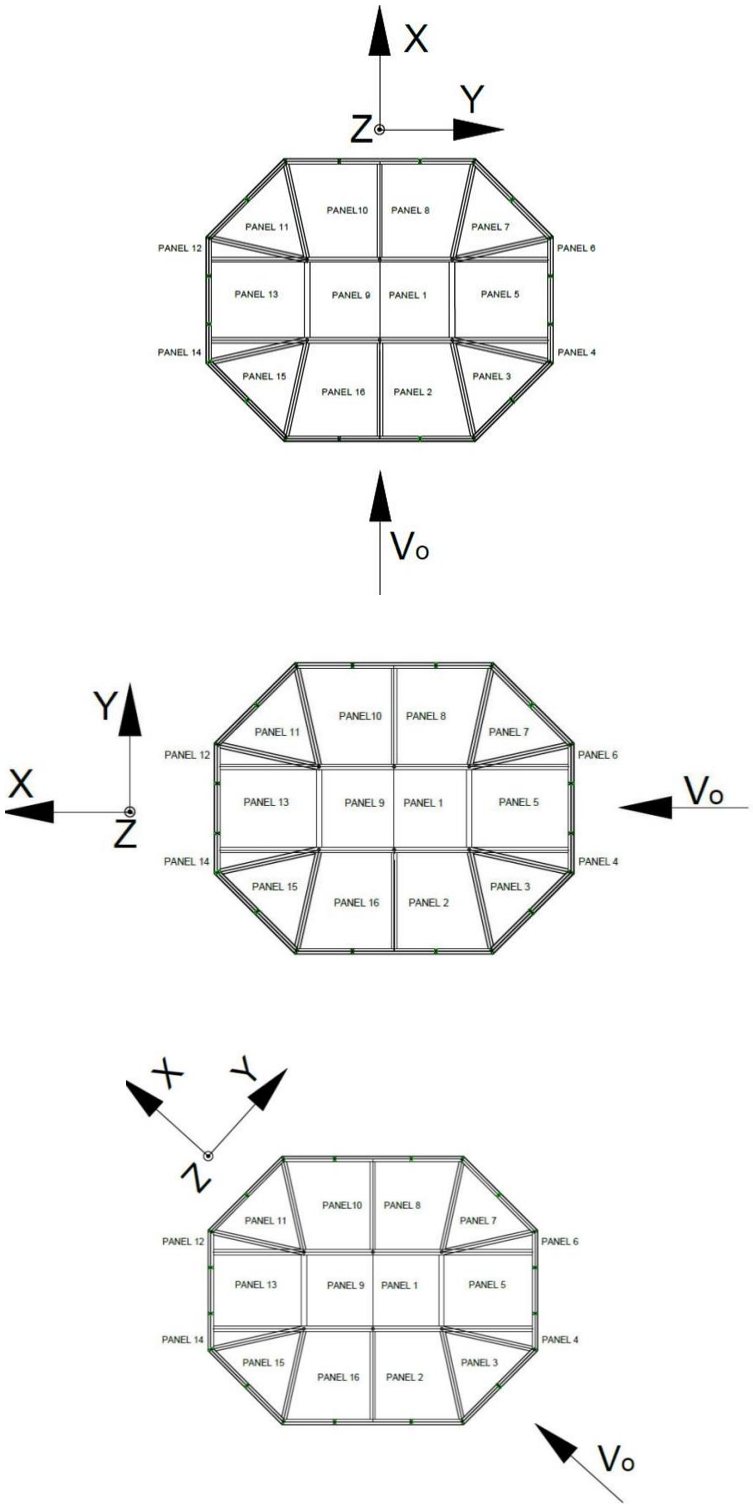

Table 2. Loads for East wind.

Panel	Closed [N/m^2]	Semi-open [N/m^2]	Open [N/m^2]
1	**1.619**	**689**	
2	**-654**	**-1157**	**-1255**
3	**-430**	**-900**	**-925**
4	**-391**	**113**	**-970**
5	**1.062**	**551**	**429**
6	**840**	**334**	**165**
7	**580**	**369**	**192**
8	**601**	**264**	**152**
9	**1.619**	**689**	
10	**601**	**264**	**152**
11	**580**	**369**	**192**
12	**840**	**334**	**165**
13	**1.062**	**551**	**429**
14	**-391**	**113**	**-970**
15	**-430**	**-900**	**-925**
16	**-654**	**-1157**	**-1255**

Table 3. Loads for North wind.

Panel	Closed [N/m^2]	Semi-open [N/m^2]	Open [N/m^2]
1	540	418	
2	419	156	-73
3	158	-20	40
4	26	-50	-69
5	82	-434	-99
6	26	-50	-69
7	158	-20	40
8	419	156	-73
9	588	810	346
10	581	445	361
11	**668**	461	488
12	643	338	479
13	472	435	488
14	643	338	361
15	**668**	461	346
16	581	445	-73

Table 4. Loads for North-East wind.

Panel	Closed [N/m^2]	Semi-open [N/m^2]	Open [N/m^2]
1	1,007	106	
2	-238	-263	699
3	214	-266	235
4	-393	-253	620
5	502	-13	66
6	1,330	400	-603
7	474	89	-160
8	522	141	-257
9	1,135	311	275
10	540	384	344
11	405	446	194
12	330	435	177
13	843	290	-38
14	231	-12	78
15	410	167	-231
16	236	-77	699

3.3 Alternative configuration

In previous measurements the roof was all sealed. Then an alternative solution was implemented. In a second experiment, the glass panels that closed the gaps between the arc structure which supports the sliding roof and the lower roof (Figure 6), were removed. The glass wall, which closed the gap under the arc, were taken out in order to get air passing under the roof. Figure 12 shows the ΔC_p distribution over the roof for the different wind directions.

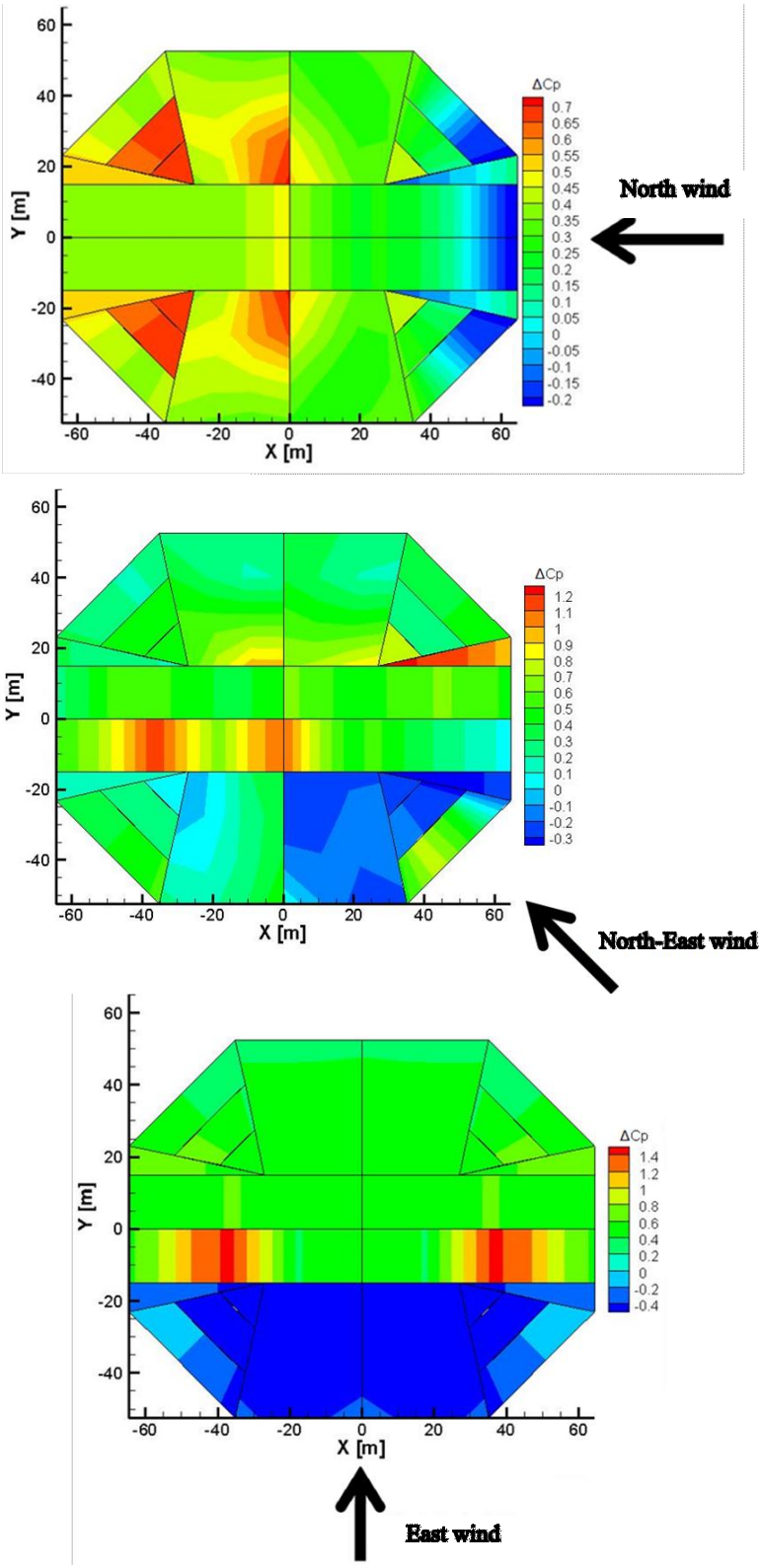

Figure 12. ΔC_p distribution without glass panels for the closed roof.

In Table 5 we show the resultant loads for the alternative case. If we compare the results obtained in this case with those measured previously, an important difference in values can be seen in panels 1 and 9. We found an important reduction in the loads, as is shown in Table 6.

Table 5. Load for the alternative solution.

Panel	North wind [N/m^2]	North-East wind [N/m^2]	East wind [N/m^2]
1	**361**	**743**	**575**
2	419	-238	-654
3	158	214	-430
4	26	-393	-391
5	82	502	1,062
6	26	1,330	840
7	158	474	580
8	419	522	601
9	**484**	**734**	**575**
10	581	540	601
11	668	405	580
12	643	330	840
13	472	843	1,062
14	643	231	-391
15	668	410	-430
16	581	236	-654

Table 6. Panel loads reduction for the different wind directions.

Wind direction	Panels	
	1	**9**
North	33%	18%
North-East	26%	35%
East	65%	65%

4 CONCLUSIONS

Pressure distributions and local loads on a tennis stadium model roof with a sliding section have been measured in wind tunnel tests and have been analyzed for different wind directions and opening conditions. Through flow visualizations it was found that the open roof produces an upward flow of the wind that enters the gap between the roof and the stadium. This upward flow enhances the flow detachment above the structure. In general, the roof opening lowers the maximum local pressure loads on the roof, but, depending on flow direction, opening the roof can increase local loads on some sections.

An alternative solution, leaving open vertical gap at both sides of the roof, leads to an important load reduction, up to 65 % for some roof panels.

ACKNOWLDEGEMENTS

The authors are grateful to Eng. Sebastián Hernández, Eng. Gonzalo Alasia and Eng. Victor Padilla for his help at the model construction and the wind tunnel tests.

REFERENCES

[1] CIRSOC 102. *Reglamento Argentino de acción del viento sobre las construcciones*, INTI, Argentina. 2005

[2] Biagini P., Borri C. ,Facchini L. Wind response of large roofs of stadions and arena. J. Wind Eng. Ind. Aerodyn 95 pp. 871–887, 2007.

[3] Cook, N.J., Mayne, J.R. A refined working approach to the assessment of wind loads for equivalent static design. J. Wind Eng. Ind. Aerodyn. 6, 125–137, 1980.